Characterization of α-synuclein oligomers formed in the presence of lipid vesicles

Anvesh K.R. Dasari [a], Urmi Sengupta [b], Elizabeth Viverette [c], Mario J. Borgnia [c], Rakez Kayed [b], Kwang Hun Lim [a,*]

[a] *Department of Chemistry, East Carolina University, Greenville, NC, 27858, USA*
[b] *Departments of Neurology, Neuroscience and Cell Biology, University of Texas Medical Branch, Galveston, TX, 77555, USA*
[c] *Genome Integrity and Structural Biology Laboratory, National Institute of Environmental Health Sciences, National Institutes of Health, Department of Health and Human Services, Research Triangle Park, NC, 27709, USA*

ARTICLE INFO

ABSTRACT

Aggregation of α-synuclein into oligomers and fibrils is associated with numerous neurodegenerative diseases such as Parkinson's disease (PD). Although the identity of the pathogenic species formed during the aggregation process is still under active debate, mounting evidence suggests that small oligomeric species rather than fibrillar aggregates are real toxic species. Isolation and characterization of small oligomers is essential to developing therapeutic strategies to prevent oligomer formation. Preparation of misfolded oligomeric species for biophysical characterization is, however, a great challenge due to their heterogenous, transient nature. Here we report the preparation of toxic and non-toxic α-synuclein oligomeric species formed at different pH values in the presence of lipid vesicles that mimic mitochondria membranes containing cardiolipin. Biophysical characterization of the lipid-induced α-synuclein oligomeric assemblies revealed that α-synuclein oligomers formed at pH 7.4 have higher surface hydrophobicity than the aggregates formed at pH 6.0. In addition, the high-pH oligomers were shown to exhibit higher toxicity than the low-pH aggregates. Structural, dynamic properties of the oligomers were also investigated by using circular dichroism (CD) and NMR spectroscopy. Our CD analyses revealed that the two oligomeric species have distinct molecular conformations, and 2D ^{1}H/^{15}N HSQC NMR experiments suggested that the high-pH oligomers have more extended dynamic regions than the low-pH aggregates. The distinct structural and dynamic properties of the oligomers might be associated with their different cytotoxic properties.

1. Introduction

Biophysical characterization of misfolded oligomeric intermediate states is critical to not only understanding the molecular mechanism of misfolding and aggregation process, but also developing therapeutic agents and biomarkers. Preparation of well-defined oligomeric species is a prerequisite for biophysical studies. The sample preparation is, however, of an enormous challenge because misfolding and aggregation can take place via multiple misfolding pathways, leading to the formation of diverse oligomers [1–5]. Misfolding and aggregation of α-synuclein is also affected by a variety of factors such as metal ions, negatively charged lipids, other aggregation-prone proteins including β-amyloid and tau, and DNA [6–10]. Interaction between α-synuclein and diverse cofactors in cellular environments may play an important role in

promoting misfolding and aggregation of α-synuclein in vivo, which may result in the formation of diverse α-synuclein aggregates in vivo [11,12]. Our recent cryo-EM structural studies revealed that the microtubule-associated protein, tau, promotes the formation of homogeneous α-synuclein filaments, suggesting that interaction between α-synuclein and tau directs the protein to a specific misfolding pathway [13]. We, therefore, hypothesized that each cofactor might induce the formation of distinct, homogeneous oligomers by promoting misfolding and aggregation through a specific misfolding pathway.

In this study, phospholipid vesicles that mimic mitochondria membranes were chosen for the cofactor because α-synuclein localizes to the mitochondria, which might be associated with mitochondria dysfunction [14–16]. Mitochondria membranes are unique in that they contain negatively charged cardiolipin (CL) [17] and the α-synuclein/CL interaction was shown to play important roles in α-synuclein aggregation and

Abbreviations

PD	Parkinson's disease
CD	circular dichroism
HSQC	heteronuclear single-quantum coherence
DOPC	1,2-Dioleoyl-sn-glycero-3-phosphocholine
DOPE	1,2-dioleoyl-sn-glycero-3-phosphoethanolamine
CL	cardiolipin
TEM	transmission electron microscopy
DLB	dementia with Lewy bodies
ThT	thioflavin T
DLS	Dynamic light scattering
ANS	8-anilino-1-naphthalenesulfon- ic acid
MTT	3-(4,5-dimethylthiazol-2-yl)-2,5-diphenyltetrazolium bromide

mitochondria dysfunction [18–22]. Thus, lipid vesicles containing CL were used to prepare diverse α-synuclein oligomeric species at different pH values since the aggregation property of α-synuclein is significantly affected by pH.

2. Material and methods

2.1. α-synuclein expression and purification

Plasmid pET21a (a gift from Michael J Fox Foundation, Addgene plasmid # 51,486) containing full-length human α-synuclein was transformed into BL21 (DE3) *E. coli* cells and expressed in LB medium as described previously [23]. Briefly, *E. coli* cultures were grown in LB medium containing carbenicillin (100 μg/mL) at 37 °C. α-Synuclein expression was induced when OD_{600} reached 0.8 by adding 0.5 mM IPTG. After 12 h of incubation at 25 °C, cells were collected via centrifugation. The cell pellet was resuspended in lysis buffer (20 mM Tris, 150 mM NaCl, pH 8.0) and sonicated. The sonicated *E. coli* was centrifuged at 12,500 rpm at 4 °C for 30 min. The soluble fraction of the cell lysate was precipitated with 50 % (w/v) $(NH_4)_2SO_4$ at 4 °C, then centrifuged. The resultant protein pellet was resuspended in dialysis buffer (10 mM tris buffer, 2 mM EDTA, pH 8.0) and dialyzed against the same buffer overnight at 4 °C. α-synuclein was further purified by anion exchange chromatography (HiTrap Q HP; 20 mM tris buffer, pH 8) followed by gel filtration (HiLoad 16/60 Superdex 75 pg) at 4 °C.

2.2. Preparation of lipid vesicles

The lipid vesicles were prepared by hydrating the dried lipid mixture (DOPC:DOPE:CL with a molar ratio of 2.0:1.3:1.0) with 10 mM phosphate buffer (pH 6.5) and by stirring the mixture using a vortex mixer (Fisher Scientific) for 2 h at 45 °C. The hydrated lipid suspension was then subjected to five freeze/thaw cycles by alternately placing the sample vial in a dry ice bath and water bath. The small unilamellar vesicles (SUVs) were prepared by extruding the lipid solution 11 times through a 0.1 μm membrane filter at 45 °C.

2.3. Dynamic Light scattering (DLS)

The size distribution of lipid vesicles was determined by using the DynaPro NanoStar DLS equipment. A 10 μL of lipid vesicle suspension was added to a quartz cuvette, and DLS measurements were recorded with an acquisition time of 3 s using a laser wavelength of 658 nm.

2.4. Preparation of α-synuclein aggregates

Monomeric α-synuclein (60 μM) was incubated with lipid vesicles

(100 μM) at different pHs (7.4–6.0) at 37 °C under the quiescent condition. After four weeks of incubation, the protein solution containing α-synuclein oligomers was concentrated by 10–20 times using a 50 kDa Centriprep centrifugal filter and the oligomers were precipitated out with 15 % ammonium sulfate. The resultant α-synuclein oligomers were collected by centrifugation at 4 °C.

2.5. Aggregation assay

The α-synuclein aggregation kinetics were monitored by measuring ThT fluorescence using a SpectraMax® microplate reader. Monomeric α-synuclein (60 μM) was incubated with or without lipid vesicles (100 μM) in the presence of 50 μM thioflavin T (ThT). A 200 μL of each sample was added in duplicates to a 96-well black clear bottom microplate and sealed airtight. Microplates were incubated at 37 °C under the quiescent condition, and the ThT fluorescence emission was monitored at 482 nm with an excitation of 440 nm.

2.6. Negative staining transmission electron microscopy (TEM)

Carbon-coated formvar copper 300 mesh grids were glow discharged. A 5 μL of the α-synuclein sample was placed onto the grid and incubated for 30 s. The excess sample was blotted off with a filter paper, and the grids were washed with distilled water. The samples were then negatively stained using 1% uranyl acetate for 30 s. The excess sample was blotted off again, and the grids were air-dried. The samples were imaged with a Philips CM12 transmission electron microscope at an accelerating voltage of 80 kV.

2.7. Circular dichroism (CD) spectroscopy

CD spectra of α-synuclein oligomers (10 μM) formed in the presence of lipid vesicles were acquired on a Jasco 815 spectrometer using a 0.1 cm pathlength quartz cuvette. The α-synuclein oligomeric sample (0.2 mg/mL) in 10 mM phosphate buffer was added to the cuvette, and an average of 30 scans was acquired for each sample.

2.8. -Anilino-1-naphthalenesulfonic acid (ANS) fluorescence

The α-synuclein oligomers (10 μM) were mixed with ANS working solution (20 μM in 10 mM phosphate buffer). The ANS fluorescence was measured on a Horiba PTI QuantaMaster 400 using excitation and emission wavelengths of 350 nm and 410–570 nm, respectively, with a 1 mm slit-width.

2.9. Cell viability assay

Cell cytotoxicity was measured in duplicates for each sample using the Invitrogen CyQUANT MTT Cell Viability Assay kit. The SH-SY5Y cells were grown in DMEM/F12 (1:1) medium with 10% FBS and 1% Pen-Strep at 37 °C. The cells were plated at a density of 10,000 cells/well in a clear bottom 96-well black plate and allowed to attach to the surface for one day. The cells were then treated with α-synuclein oligomers at concentrations of 10 and 40 μM and incubated for 48 h at 37 °C. MTT was then added to the culture medium to a final concentration of 0.5 mg/ml and incubated for 4 h. SDS was added to the wells to a final concentration of 50 mg/mL and incubated at 37 °C. After 4 h of incubation, the absorbance was measured at 570 nm. Cell viability was reported relative to the control cells exposed to only the cell medium.

2.10. Solution-state NMR

The ^{15}N-labeled α-synuclein oligomers were prepared by incubating monomeric α-synuclein (60 μM) with CL-containing lipid (100 μM) for four weeks. The α-synuclein oligomers were concentrated 10–20 times using a 50 kDa membrane filter. 2D $^1H/^{15}N$ HSQC NMR spectra of

α-synuclein oligomers were acquired on an 800 MHz 52 mm Bruker NMR spectrometer equipped with a cryoprobe.

2.11. Cryo-EM

A 3 μL sample of α-synuclein oligomers was applied to a glow discharged R2/1 Quantifoil grid and blotted with a filter paper at 4 °C and 95 % humidity. The grids were plunge frozen using the Leica EM GP2 automatic plunge freezer. The electron micrographs were obtained using a Talos Arctica electron microscope operated at 200 kV equipped with a GATAN K2 Summit DED. Images were acquired at a nominal magnification of 45,000 ×. Movies were collected as a series of 60 frames at a dose rate of 0.6 e⁻/Å²/s over 9 s. Beam-induced motions were corrected, and dose weighting was performed using MotionCor2 [24]. Contrast transfer function (CTF) estimation was performed using CTFFind4 [25].

3. Results

α-synuclein aggregation was monitored in the presence of lipid vesicles that mimic mitochondria inner membranes (DOPC:DOPE:CL with a molar ratio of 2.0:1.3:1.0) [17] at different pH values (Fig. 1a). The thioflavin T (ThT) fluorescence assay was used to examine aggregation kinetics in the presence and absence of the lipid vesicles. Under the quiescent condition, ThT fluorescence increased after several days of incubation with the lipid vesicles (solid lines), while notable enhancement was observed only after longer incubations without the lipid vesicles (dotted lines). The ThT aggregation assay revealed that the lipid vesicles with negatively charged CL promote α-synuclein aggregation, and the aggregation of α-synuclein is accelerated under more acidic conditions (red, blue, and green in Fig. 1a).

Transmission electron microscopy (TEM) was used to examine the morphology of the α-synuclein aggregates formed in the presence of the lipid vesicles (Fig. 1b). The TEM images reveal that WT α-synuclein forms small oligomeric species at the neutral pHs of 6.5–7.4. Slightly bigger aggregates were also observed at a lower pH of 6.0. Fibrillar aggregates were, however, not observed in the α-synuclein aggregates formed under these conditions. The α-synuclein oligomers are most likely to be in equilibrium with monomers. For the biophysical characterization, the misfolded oligomers should be separated from the native monomers. In our previous studies, we demonstrated that small misfolded transthyretin (TTR) oligomers with a diameter of ~5–6 nm could be extracted from the native TTR using a smaller amount of ammonium sulfate than that needed for native TTR because misfolded oligomers must have higher aggregation propensity [26].

In order to isolate the α-synuclein oligomeric species using ammonium sulfate, the incubated protein solution (60 μM) was concentrated by 10–20 times using 50 kDa cutoff membrane filters, and 15 % ammonium sulfate was used to extract the oligomeric species (α-synuclein monomers begin to precipitate with 35–40 % ammonium sulfate). The oligomer samples remain stable even after being concentrated by 10–20 times (Figs. S1a and S1b), and the precipitates also consist of the oligomeric species (Fig. S1c), which will allow for the structural characterization of the oligomers.

Cytotoxic activities of the oligomers were examined using MTT (3-(4,5-dimethylthiazol-2-yl)-2,5-diphenyltetrazolium bromide) assay on human neuroblastoma SH-SY5Y cells (Fig. 2a). Notably, the high-pH oligomers (brown) are more toxic than the low-pH aggregates (blue). The cytotoxicity of the oligomers was shown to be correlated well with their hydrophobicity [27]. Thus, ANS (8-Anilinonaphthalene-1-sulfonic acid) fluorescence assay was used to compare the hydrophobicity of the high- and low-pH oligomers (Fig. 2b). The high-pH oligomers exhibit higher surface hydrophobicity than the low-pH aggregates, which is correlated well with the toxicity.

Structural features of the oligomers obtained by precipitation with 15 % ammonium sulfate were investigated using CD spectroscopy (Fig. 3). The CD spectra reveal that the oligomers formed at the higher pH values (7.4 and 6.5) have helical characters considering the substantial intensity at ∼ 210 nm (Table S1). The α-helical amyloidogenic intermediates have been previously observed during misfolding and aggregation process [28–31]. On the other hand, oligomeric species formed at the lower pH value have less helical characters, suggesting that the non-toxic, low pH oligomers adopt different conformations from those of the toxic high pH oligomers.

Misfolded oligomers contain both structured, core regions and more dynamic, disordered regions. The more flexible regions in the oligomers can be probed by solution NMR spectroscopy. Fig. 4 shows solution NMR spectra of the α-synuclein oligomers formed in the presence of the lipid vesicles. The overlaid 2D ^{1}H/^{15}N HSQC NMR spectra of the monomeric (black) and oligomeric (red and green) α-synuclein reveal distinct cross-peaks of the high- (red) and low- (green) pH oligomeric species from those of the native monomers. The distinct cross-peaks from the oligomeric species clearly indicate that the oligomers adopt different molecular conformations from the monomers (black). It is also interesting to note that the oligomer cross-peaks with distinct chemical shifts from those of the monomers have narrow linewidths comparable to those of the monomer cross-peaks. The narrow NMR cross-peaks from the oligomers suggest that the oligomers have highly flexible regions.

The overlaid HSQC spectra also reveal distinct cross-peaks from the two oligomers (red and green), suggesting that the two oligomers have different disordered regions. Notably, much fewer cross-peaks were detected for the non-toxic, low-pH aggregates (green), consistent with the bigger aggregates observed for the low-pH oligomers (Fig. 1b). The size of the oligomers might be related to the different toxicity, as was previously observed [27]. It is also interesting to note the cross-peaks at unusual chemical shifts (7.5–8.0 ppm, 125–130 ppm) in the ^{1}H–^{15}N HSQC spectrum for the high-pH oligomers (red). The narrow NMR cross-peaks similar to those of the disordered monomer (black) suggest that the NMR resonances originate from flexible regions. However, the chemical shifts of the cross-peaks are distinct from those of the disordered states (black), suggesting that those regions in the high-pH oligomer may have distinct residual structures.
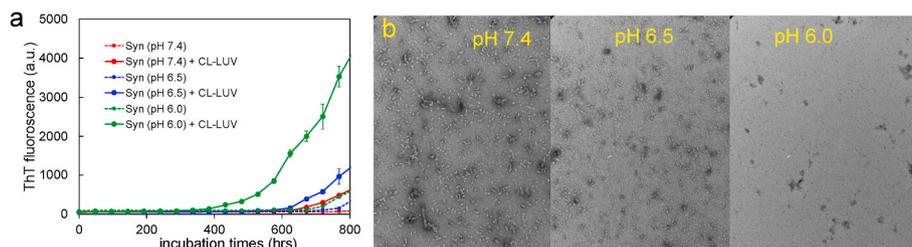
Fig. 1. (a) Aggregation kinetics of WT α-synuclein (60 μM) in the presence of the lipid vesicles (100 μM) with a diameter of 100 nm monitored by thioflavin T (ThT) fluorescence at different pHs (7.4–6.0) and 37 °C under the quiescent condition. (b) TEM images of the α-synuclein oligomers formed in the presence of the lipid vesicles at the different pHs for four weeks. Fibrillar aggregates were not observed for the three incubated solutions. The ThT fluorescence emission was monitored at 482 nm with an excitation of 440 nm.
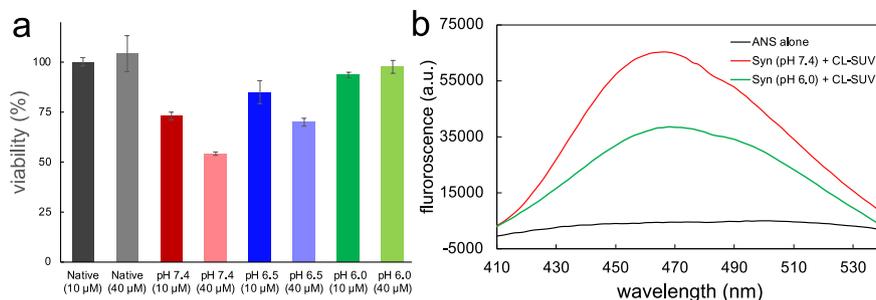
Fig. 2. (a) Cell viability measured using MTT assay for the native α-synuclein monomers and oligomers formed in the presence of the lipid vesicles at different pHs. (b) ANS fluorescence intensity for the high- (red) and low- (green) pH oligomers. The SH-SY5Y cells were treated with the protein assemblies, and the biochemical assays were carried out after 48 h of incubations at 37 °C.
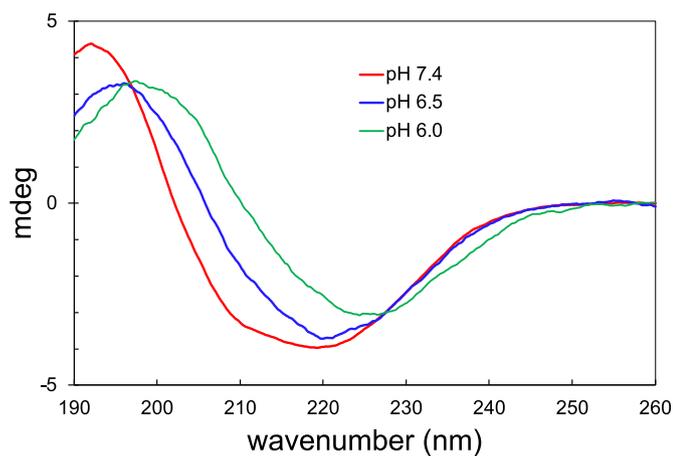
Fig. 3. CD spectra of the oligomers formed in the presence of the CL-SUVs at different pHs. Oligomers precipitated by 15 % ammonium sulfate were resuspended with PBS buffer to a final concentration of 0.2 mg/ml. An average of 30 scans was acquired for each sample.

4. Discussion

Preparation of toxic and non-toxic oligomers, and subsequent biophysical characterization of the oligomers are critically important to understanding the cytotoxic nature of the misfolded oligomers and to developing therapeutic agents to inhibit their pathogenic activities. Although the molecular mechanism of oligomer formation in cellular environments has remained elusive, extensive previous studies revealed that various cofactors can trigger misfolding and aggregation in vitro. Indeed, diverse α-synuclein oligomers with different sizes were prepared by the cofactors, suggesting that the cofactors in cellular environments may play a critical role in α-synuclein aggregation in vivo [32]. In this study, lipid vesicles with the mitochondria membrane composition were used to prepare α-synuclein oligomers. Our biophysical analyses revealed that the lipid vesicles induce the formation of small oligomers with a diameter of ~4–5 nm at pH 6.5–7.4 (Fig. S2), and the small oligomers appear to self-assemble into bigger oligomeric species (Fig. 1b). The small and bigger α-synuclein oligomers in equilibrium at pH 7.4 exhibited higher surface hydrophobicity and stronger toxicity than α-synuclein aggregates formed at a lower pH of 6.0. Structural characterization of the oligomers using CD and NMR showed that the two types of oligomers formed at pH 7.4 and 6.0 have distinct molecular conformations, which might be associated with their different cytotoxicity.

The cytotoxic properties of the lipid-induced α-synuclein oligomers are generally consistent with previous studies of misfolded oligomers. Firstly, previous studies revealed that surface hydrophobicity is
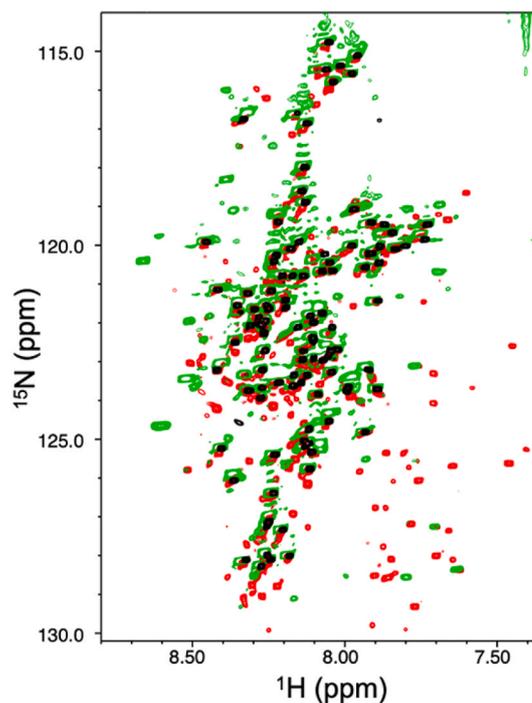
Fig. 4. Overlaid 2D ^{1}H/^{15}N HSQC NMR spectra for α-synuclein monomers (black), α-synuclein oligomers formed at pH 7.4 (red) and 6.0 (green) acquired using 800 MHz NMR at 15 °C. The protein solution (60 μM) incubated for four weeks was concentrated by 10–20 times using a 50 kDa membrane filter to increase the concentration of the oligomers. Sixty-four FIDs were accumulated for each sample.

correlated well with the toxicity of misfolded oligomers derived from α-synuclein and β-amyloid (Aβ) peptides [27]. These results indicate that the extent of the exposed hydrophobic surface is a key parameter for toxic misfolded oligomers. The hydrophobic surface of the oligomers may play critical roles in cellular dysfunctions through aberrant interactions with lipid membranes and various cellular proteins involved in signaling pathways. Secondly, smaller misfolded oligomeric species were shown to exhibit higher toxicity, and larger assemblies, including fibrils, appeared to reduce toxicity [27,33,34]. Our TEM images of the oligomers also revealed that bigger aggregates were observed in the less toxic oligomers formed at pH 6.0, and fewer cross-peaks were detected in the NMR spectrum for the low-pH aggregates presumably due to their larger size. The smaller misfolded oligomers with more flexible regions may diffuse more easily inside the cells, interfering with cellular functions more effectively.

In summary, we demonstrated that α-synuclein oligomers with

different cytotoxic properties can be prepared by utilizing lipid vesicles mimicking mitochondria membranes. The more toxic oligomers formed at the physiological pH exhibited distinct structural, dynamic properties from those of non-toxic aggregates, which might be associated with higher surface hydrophobicity of the toxic oligomers. More detailed structural characterization of the toxic oligomers will provide valuable insights into the cytotoxic nature of the misfolded oligomers.

Funding sources

Notes

The authors declare no competing financial interest.

CRediT authorship contribution statement

Anvesh K.R. Dasari: Writing – original draft, Investigation. **Urmi Sengupta:** Resources, Investigation. **Elizabeth Viverette:** Investigation. **Mario J. Borgnia:** Writing – review & editing, Resources, Methodology. **Rakez Kayed:** Writing – review & editing, Methodology, Investigation. **Kwang Hun Lim:** Writing – review & editing, Writing – original draft, Investigation, Conceptualization.

Declaration of competing interest

The authors declare that they have no known competing financial interests or personal relationships that could have appeared to influence the work reported in this paper.

Data availability

Data will be made available on request.

Appendix A. Supplementary data

Supplementary data to this article can be found online at https://doi.org/10.1016/j.bbrep.2024.101687.

References

[1] J.S. Pedersen, C.B. Andersen, D.E. Otzen, Amyloid structure–one but not the same: the many levels of fibrillar polymorphism, FEBS J. 277 (2010) 4591–4601.

[2] K. Annamalai, A.H. Guhrs, R. Koehler, M. Schmidt, H. Michel, C. Loos, P. M. Gaffney, C.J. Sigurdson, U. Hegenbart, S. Schonland, M. Fandrich, Polymorphism of amyloid fibrils in vivo, Angew. Chem., Int. Ed. Engl. 55 (2016) 4822–4825.

[3] H. Heise, W. Hoyer, S. Becker, O.C. Andronesi, D. Riedel, M. Baldus, Molecular-level secondary structure, polymorphism, and dynamics of full-length alpha-synuclein fibrils studied by solid-state NMR, in: Proceedings of the National Academy of Sciences of the United States of America vol. 102, 2005, pp. 15871–15876.

[4] R. Kodali, R. Wetzel, Polymorphism in the intermediates and products of amyloid assembly, Curr. Opin. Struct. Biol. 17 (2007) 48–57.

[5] T. Eichner, S.E. Radford, A diversity of assembly mechanisms of a generic amyloid fold, Mol. Cell. 43 (2011) 8–18.

[6] A.D. Stephens, M. Zacharopoulou, G.S. Kaminski Schierle, The cellular environment Affects monomeric α-synuclein structure, Trends Biochem. Sci. 44 (2019) 453–466.

[7] B.I. Giasson, M.S. Forman, M. Higuchi, L.I. Golbe, C.L. Graves, P.T. Kotzbauer, J. Q. Trojanowski, V.M. Lee, Initiation and synergistic fibrillization of tau and alpha-synuclein, Science 300 (2003) 636–640.

[8] T.I. Kam, X. Mao, H. Park, S.C. Chou, S.S. Karuppagounder, G.E. Umanah, S.P. Yun, S. Brahmachari, N. Panicker, R. Chen, S.A. Andrabi, C. Qi, G.G. Poirier, O. Pletnikova, J.C. Troncoso, L.M. Bekris, J.B. Leverenz, A. Pantelyat, H.S. Ko, L. S. Rosenthal, T.M. Dawson, V.L. Dawson, Poly(ADP-ribose) drives pathologic α-synuclein neurodegeneration in Parkinson's disease, Science 362 (2018) eaat8407, https://doi.org/10.1126/science.aat8407.

[9] C. Galvagnion, A.K. Buell, G. Meisl, T.C. Michaels, M. Vendruscolo, T.P. Knowles, C.M. Dobson, Lipid vesicles trigger α-synuclein aggregation by stimulating primary nucleation, Nat. Chem. Biol. 11 (2015) 229–234.

[10] U. Sengupta, N. Puangmalai, N. Bhatt, S. Garcia, Y. Zhao, R. Kayed, Polymorphic α-synuclein strains modified by dopamine and docosahexaenoic acid interact differentially with tau protein, Mol. Neurobiol. 57 (2020) 2741–2765.

[11] T. Strohäker, B.C. Jung, S.H. Liou, C.O. Fernandez, D. Riedel, S. Becker, G. M. Halliday, M. Bennati, W.S. Kim, S.J. Lee, M. Zweckstetter, Structural heterogeneity of α-synuclein fibrils amplified from patient brain extracts, Nat. Commun. 10 (2019) 5535, w.

[12] S.H. Shahmoradian, A.J. Lewis, C. Genoud, J. Hench, T.E. Moors, P.P. Navarro, D. Castaño-Díez, G. Schweighauser, A. Graff-Meyer, K.N. Goldie, R. Sütterlin, E. Huisman, A. Ingrassia, Y. Gier, A.J.M. Rozemuller, J. Wang, A. Paepe, J. Erny, A. Staempfli, J. Hoernschemeyer, F. Großerüschkamp, D. Niedieker, S.F. El-Mashtoly, M. Quadri, W.F.J. Van Ijcken, V. Bonifati, K. Gerwert, B. Bohrmann, S. Frank, M. Britschgi, H. Stahlberg, W.D.J. Van de Berg, M.E. Lauer, Lewy pathology in Parkinson's disease consists of crowded organelles and lipid membranes, Nat. Neurosci. 22 (2019) 1099–1109.

[13] A. Hojjatian, A.K.R. Dasari, U. Sengupta, D. Taylor, N. Daneshparvar, F. A. Yeganeh, L. Dillard, B. Michael, R.G. Griffin, M.J. Borgnia, R. Kayed, K. A. Taylor, K.H. Lim, Tau induces formation of α-synuclein filaments with distinct molecular conformations, Biochem. Biophys. Res. Commun. 554 (2021) 145–150.

[14] S. Mullin, A. Schapira, α-Synuclein and mitochondrial dysfunction in Parkinson's disease, Mol. Neurobiol. 47 (2013) 587–597.

[15] L.J. Hsu, Y. Sagara, A. Arroyo, E. Rockenstein, A. Sisk, M. Mallory, J. Wong, T. Takenouchi, M. Hashimoto, E. Masliah, Alpha-synuclein promotes mitochondrial deficit and oxidative stress, Am. J. Pathol. 157 (2000) 401–410.

[16] S.J. Chinta, J.K. Mallajosyula, A. Rane, J.K. Andersen, Mitochondrial α-synuclein accumulation impairs complex I function in dopaminergic neurons and results in increased mitophagy in vivo, Neurosci. Lett. 486 (2010) 235–239.

[17] G. van Meer, D.R. Voelker, G.W. Feigenson, Membrane lipids: where they are and how they behave, Nat. Rev. Mol. Cell Biol. 9 (2008) 112–124.

[18] S. Ghio, A. Camilleri, M. Caruana, V.C. Ruf, F. Schmidt, A. Leonov, S. Ryazanov, C. Griesinger, R.J. Cauchi, F. Kamp, A. Giese, N. Vassallo, Cardiolipin promotes pore-forming activity of alpha-synuclein oligomers in mitochondrial membranes, ACS Chem. Neurosci. 10 (2019) 3815–3829.

[19] M. Falabella, H.J. Vernon, M.G. Hanna, S.M. Claypool, R.D.S. Pitceathly, Cardiolipin, mitochondria, and neurological disease, Trends Endocrinol. Metabol. 32 (2021) 224–237.

[20] T. Ryan, V.V. Bamm, M.G. Stykel, C.L. Coackley, K.M. Humphries, R. Jamieson-Williams, R. Ambasudhan, D.D. Mosser, S.A. Lipton, G. Harauz, S.D. Ryan, Cardiolipin exposure on the outer mitochondrial membrane modulates α-synuclein, Nat. Commun. 9 (2018) 817–819.

[21] V. Gilmozzi, G. Gentile, M.P. Castelo Rueda, A.A. Hicks, P.P. Pramstaller, A. Zanon, M. Lévesque, I. Pichler, Interaction of alpha-synuclein with lipids: mitochondrial cardiolipin as a critical player in the pathogenesis of Parkinson's disease, Front. Neurosci. 14 (2020) 578993.

[22] I.G. Zigoneanu, Y.J. Yang, A.S. Krois, E. Haque, G.J. Pielak, Interaction of α-synuclein with vesicles that mimic mitochondrial membranes, Biochim. Biophys. Acta 1818 (2012) 512–519.

[23] M. Ghee, R. Melki, N. Michot, J. Mallet, PA700, the regulatory complex of the 26S proteasome, interferes with alpha-synuclein assembly, FEBS J. 272 (2005) 4023–4033.

[24] S.Q. Zheng, E. Palovcak, J. Armache, K.A. Verba, Y. Cheng, D.A. Agard, MotionCor2: anisotropic correction of beam-induced motion for improved cryo-electron microscopy, Nat. Methods 14 (2017) 331–332.

[25] A. Rohou, N. Grigorieff, CTFFIND4: fast and accurate defocus estimation from electron micrographs, J. Struct. Biol. 192 (2015) 216–221.

[26] A.K.R. Dasari, R.M. Hughes, S. Wi, I. Hung, Z. Gan, J.W. Kelly, K.H. Lim, Transthyretin aggregation pathway toward the formation of distinct cytotoxic oligomers, Sci. Rep. 9 (2019) 33, 1.

[27] B. Mannini, E. Mulvihill, C. Sgromo, R. Cascella, R. Khodarahmi, M. Ramazzotti, C. M. Dobson, C. Cecchi, F. Chiti, Toxicity of protein oligomers is rationalized by a function combining size and surface hydrophobicity, ACS Chem. Biol. 9 (2014) 2309–2317.

[28] V.L. Anderson, T.F. Ramlall, C.C. Rospigliosi, W.W. Webb, D. Eliezer, Identification of a helical intermediate in trifluoroethanol-induced alpha-synuclein aggregation, Proc. Natl. Acad. Sci. U.S.A. 107 (2010) 18850–18855.

[29] A. Abedini, D.P. Raleigh, A role for helical intermediates in amyloid formation by natively unfolded polypeptides? Phys. Biol. 6 (2009), 015005-3975/6/1/015005.

[30] K.H. Lim, Y.T. Le, H.H. Collver, C. Putnam-Evans, J.M. Kenney, Characterization of amyloidogenic intermediate states through a combined use of CD and NMR spectroscopy, Biophys. Chem. 151 (2010) 155–159.

[31] G. Comellas, L.R. Lemkau, D.H. Zhou, J.M. George, C.M. Rienstra, Structural intermediates during α-synuclein fibrillogenesis on phospholipid vesicles, J. Am. Chem. Soc. 134 (2012) 5090–5099.

[32] C. Peng, R.J. Gathagan, D.J. Covell, C. Medellin, A. Stieber, J.L. Robinson, B. Zhang, R.M. Pitkin, M.F. Olufemi, K.C. Luk, J.Q. Trojanowski, V.M. Lee, Cellular milieu imparts distinct pathological alpha-synuclein strains in alpha-synucleinopathies, Nature 557 (2018) 558–563.

[33] T. Yang, S. Li, H. Xu, D.M. Walsh, D.J. Selkoe, Large soluble oligomers of amyloid β-protein from alzheimer brain are far less neuroactive than the smaller oligomers to which they dissociate, J. Neurosci. 37 (2017) 152–163.

[34] P. Cizas, R. Budvytyte, R. Morkuniene, R. Moldovan, M. Broccio, M. Lösche, G. Niaura, G. Valincius, V. Borutaite, Size-dependent neurotoxicity of beta-amyloid oligomers, Arch. Biochem. Biophys. 496 (2010) 84–92.